Macromolecular Bioscience
www.mbs-journal.de

Horseradish Peroxidase-Crosslinked Calcium-Containing Silk Fibroin Hydrogels as Artificial Matrices for Bone Cancer Research

*Lara Pierantoni, Viviana P. Ribeiro, Lígia Costa, Sandra Pina, Alain da Silva Morais, Joana Silva-Correia, Subhas C. Kundu, Antonella Motta, Rui L. Reis, and Joaquim M. Oliveira**

Hydrogels, being capable of mimicking the extracellular matrix composition of tissues, are greatly used as artificial matrices in tissue engineering applications. In this study, the generation of horseradish peroxidase (HRP)-crosslinked silk fibroin (SF) hydrogels, using calcium peroxide as oxidizer is reported. The proposed fast forming calcium-containing SF hydrogels spontaneously undergo SF conformational changes from random coil to β-sheet during time, exhibiting ionic, and pH stimuli responsiveness. In vitro response shows calcium-containing SF hydrogels' encapsulation properties and their ability to promote SaOs-2 tumor cells death after 10 days of culturing, upon complete β-sheet conformation transition. Calcium-containing SF hydrogels' angiogenic potential investigated in an in ovo chick chorioallantoic membrane (CAM) assay, show a high number of converging blood vessels as compared to the negative control, although no endothelial cells infiltration is observed. The in vivo response evaluated in subcutaneous implantation in CD1 and nude NCD1 mice shows that calcium-containing SF hydrogels are stable up to 6 weeks after implantation. However, an increased number of dead cells are also present in the surrounding tissue. The results suggest the potential of calcium-containing SF hydrogels to be used as novel in situ therapeutics for bone cancer treatment applications, particularly to osteosarcoma.

In recent years, the development of tissue engineered 3D constructs for disease modeling has been further explored. These 3D systems can be exploited to test new potential anticancer treatments[1] or used as drug-delivery systems[2] of chemotherapeutic agents commonly used in cancer therapy, such as Doxorubicin (DOX)[3,4] and 5-FU.[5] In particular hydrogels, being capable to be finely tuned to mimic the native extracellular matrix (ECM) microenvironment, are greatly used for the generation of 3D tissue models and targeted drug-delivery systems.[6,7] Silk fibroin (SF), compared to other natural biopolymers, holds numerous advantages,[8] including the ability to undergo different processing methods to produce several types of biomaterials with modulated bioactivity.[9] In particular, silk-based biomaterials have shown promising biomedical applications in bone tissue engineering field, given their capacity to induce osteogenic signaling both in vitro and in vivo.[10] SF hydrogels have been also proposed for the development of mineralized 3D bone-mimicking constructs, and 3D in vitro tumor and bone metastasis models.[11–14]

Belonging to the family of bone cancers, osteosarcoma represents one of the most common types of primary bone malignancy affecting children and young adults.[15–17] It develops preferentially at the metaphysis of long bones, mainly the distal femur, proximal tibia, and proximal humerus.[18] At

L. Pierantoni, Dr. V. P. Ribeiro, L. Costa, Dr. S. Pina, Dr. A. da Silva Morais, Dr. J. Silva-Correia, Prof. S. C. Kundu, Prof. R. L. Reis, Dr. J. M. Oliveira
3B's Research Group
I3Bs – Research Institute on Biomaterials, Biodegradables and Biomimetics of University of Minho
Headquarters of the European Institute of Excellence on Tissue Engineering and Regenerative Medicine
AvePark, Zona Industrial da Gandra, Barco, Guimarães 4805-017, Portugal
E-mail: miguel.oliveira@i3bs.uminho.pt

The ORCID identification number(s) for the author(s) of this article can be found under https://doi.org/10.1002/mabi.202000425.

DOI: 10.1002/mabi.202000425

L. Pierantoni, Dr. V. P. Ribeiro, L. Costa, Dr. S. Pina, Dr. A. da Silva Morais, Dr. J. Silva-Correia, Prof. S. C. Kundu, Prof. R. L. Reis, Dr. J. M. Oliveira
ICVS/3B's – PT Government Associated Laboratory
Braga/ Guimarães, Portugal
Prof. A. Motta
Department of Industrial Engineering, and BIOtech Research Center
University of Trento
Trento 38123, Italy
Prof. A. Motta
European Institute of Excellence on Tissue Engineering and Regenerative Medicine
Trento Unit
Trento 38123, Italy

diagnosis, about 20% of patients present metastasis, most frequently in the lungs.[17] From a genetic point of view, osteosarcoma is generated from a series of concurrent mutations that acts to promote survival and proliferative advantages to cancer cells.[19] Moreover, osteosarcoma progression also occurs due to the interaction of tumor cells with the surrounding microenvironment, like growth factors released by the disrupted ECM and mesenchymal stem cells, highly present in the tumor microenvironment.[20] Osteosarcoma patients usually undergo 10 weeks neoadjuvant chemotherapy treatment with high-dose Methotrexate, Doxorubicin, and Cisplatin (MAP therapy), followed by surgical removal of the tumor.[18] After surgery, 17 weeks MAP adjuvant chemotherapy is continuously administered.[18] This is the standard treatment of osteosarcoma, however, several surgery-related disabilities and chemotherapy-related chronic side effects have been showing to induce discomfort and pain in patients.[18] Although innovative therapeutic solutions have been investigated,[21] it is essential to generate less invasive treatments that can better satisfy the patients' needs, and patient-specific approaches for fast-responsive treatments.

Herein, we aimed to investigate the potential of SF hydrogels as artificial matrices for bone cancer research, explicitly to osteosarcoma, as novel tools for therapeutic approaches. This was achieved through the generation of horseradish peroxidase (HRP)-crosslinked SF hydrogels (**Figure 1**a), using SF solution at 8 wt% concentration.[22] As substrate for the HRP, two different contents of calcium peroxide (CaO_2) were used, and denominated throughout the text as Ca-1 and Ca-2 (with Ca-1<Ca-2), respectively. As recently shown by Le Thi et al., CaO_2 dissolved into an aqueous solution will divide into $Ca(OH)_2$, H_2O_2, and O_2.[23] When mixed together with the SF solution containing HRP, the enzyme utilizes the H_2O_2 as a substrate to crosslinks the SF tyrosine side chains, thus leading to hydrogels formation.[24] For comparison purposes, hydrogen peroxide (H_2O_2) was used as an oxidizer for the enzymatic-crosslinking method to generate SF hydrogels. Calcium-containing SF hydrogels were characterized at multiscale levels structurally and physicochemically. The results revealed that the presence of calcium induced a fast hydrogels' gelation and helped to stabilize the SF structure, inducing a higher crystallinity. Moreover, they also possess a compacted porous internal microstructure, and are able to undergo spontaneously from SF random-coil to β-sheet conformational change over time. This change in conformation also resulted in the death of the hydrogels-encapsulated SaOs-2 osteosarcoma cells after 10 days of culturing. In ovo and in vivo implantation of calcium-containing SF hydrogels showed their capacity to inhibit angiogenesis and to induce surrounding tissue cells death, respectively.

The microstructural properties of SF hydrogels kept for 7 days at physiological conditions were characterized by Transmission electron microscopy (TEM) and cryo-scanning electron microscopy (Cryo-SEM) imaging (Figure 1b,c). From TEM images, it was possible to observe that SF presented a typical fibrillar conformation.[25] The microstructure evaluation by Cryo-SEM showed that SF hydrogels presented a different internal structure depending on the crosslinking agent. The calcium-containing SF hydrogels showed a dense network of interconnected pores, with an average pore size of 0.216 ± 0.031 μm for Ca-1 and 0.169 ± 0.023 μm for Ca-2, while the hydrogels crosslinked with H_2O_2 have larger pores (1 ± 0.087 μm).

SF hydrogels' crystalline phases were analyzed by X-ray diffraction (XRD) (Figure 1d). The calcium-containing SF hydrogels (Ca-1 and Ca-2 samples) presented a main peak in the region of 2θ = 28.8°–30.9°, that can be assigned to the β-sheet crystalline structure (type II β-turn).[26,27] An additional peak located at ≈21°, belonging to the hydrogels at day 14 post-gelation, is shown which corresponds to the β-sheet crystalline conformation of SF.[28,29] At day 1, the spectra presented a broad distribution, typical of an amorphous conformation of the hydrogels.[27,30] From day 3 onward, the peaks intensity increased, corresponding to an augmentation of the hydrogels crystallinity with time.[30] By its turn, SF hydrogels crosslinked with H_2O_2 presented a main peak at 2θ = 29° attributed to β-sheet type II phase, being more pronounced for days 10 and 14 post-gelation. Therefore, it is indicated that SF naturally undergo protein conformation transition over time, concomitant with SF structural transition from random-coil to β-sheet.[22,31] The presence of calcium seems to enhance the stability of SF protein structure, increasing SF hydrogels crystallinity, which is reflected also by the compact porosity observed by Cryo-SEM (Figure 1c).

The gelation time of SF hydrogels was evaluated through rheological analysis and the results were expressed by plotting the storage (G′, elastic component) and loss (G″, viscous component) moduli as a function of time (Figure 1e). Calcium-containing SF hydrogels undergo a faster gelation process (Ca-1, about 5.5 min; Ca-2, about 8 min) as compared to the ones crosslinked with H_2O_2, which jellified in about 12 min (Figure 1e). This phenomenon could be due to the presence of the calcium ions, which help to stabilize the SF, thus leading to a faster gelation. All the conditions then reached a stable plateau phase for both G′ and G″ moduli in less than 40 min. Peculiarly, all the hydrogel formulations showed increased G′ and G″ values and proximity of the curves after the plateau phase, from ≈40 min onward. This fact can be explained by the loss of moisture from the already-formed hydrogels inside the measuring chamber.

The capability of the hydrogels to respond to different ionic stimuli liquids (i.e., phosphate buffered saline (PBS), water, NaCl 0.154 M, and NaCl 2 M solutions) was also evaluated (Figure S1, Supporting Information). When SF hydrogels (crosslinked with H_2O_2 and CaO_2) were alternatively immersed in distilled water/PBS (Figure S1a, Supporting Information) and in NaCl 2 M/NaCl 0.154 M solutions (Figure S1b, Supporting Information), it was noticed an increase in diameter, corresponding to hydrogels' swelling, followed by shrinkage until the original dimensions of the tested samples. This phenomenon is related with the differences in the osmotic pressure established by the tested solutions.[22] These results demonstrated that the SF hydrogels studied in this work were able to respond to different ionic fluxes, by shrinking or swelling consequently, being able to adapt to diverse ionic changes occurring in the external environment.[22] The ability of SF hydrogels to respond to different pH, ranging from pH 3 to pH 10.5 was also tested (Figure 1f). The acidic pH was the most effective in originating a SF hydrogels response, inducing a high degree of hydrogels shrinkage. This phenomenon is probably caused by the lower

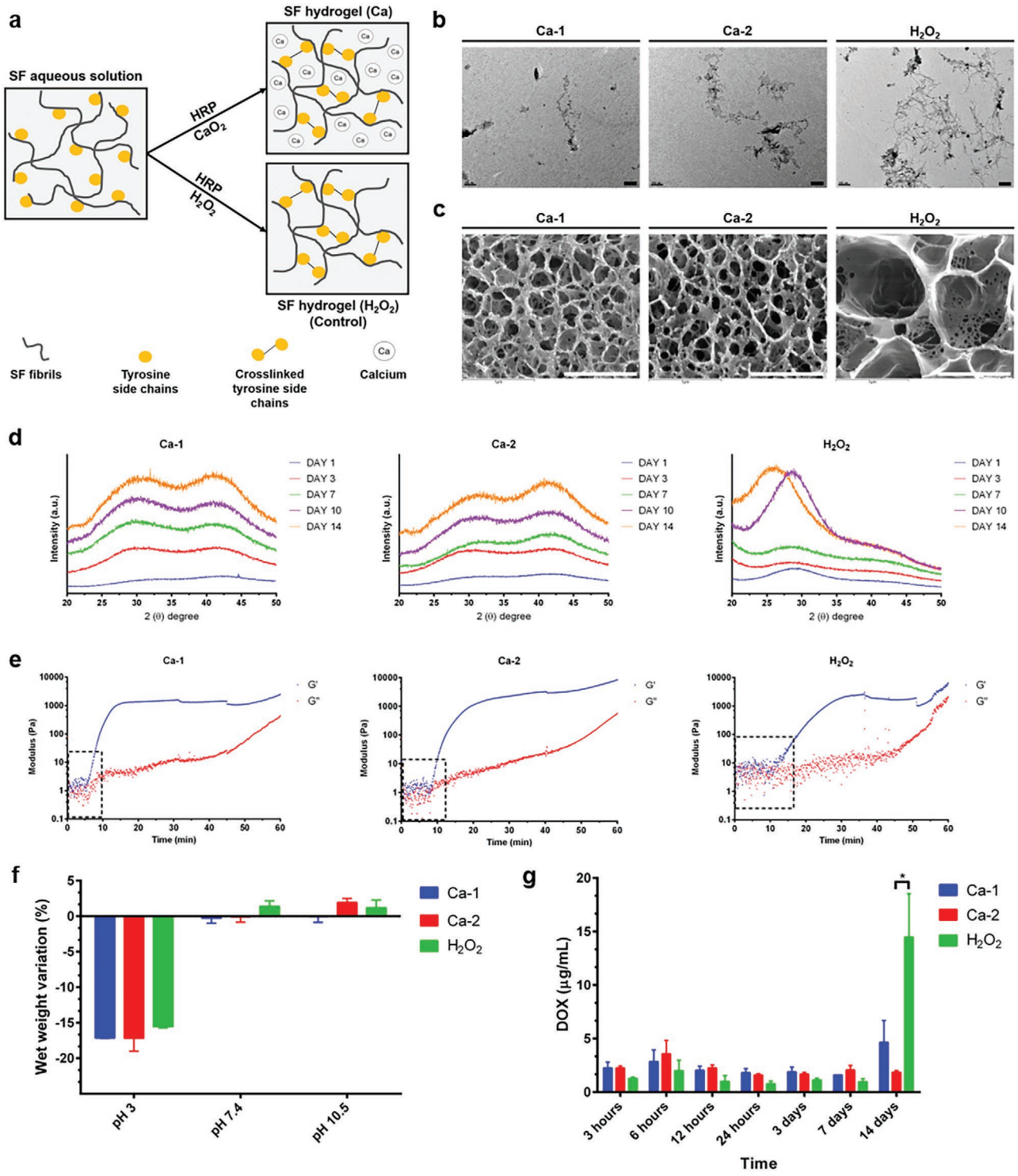

Figure 1. Structural and physicochemical characterization of HRP-crosslinked SF hydrogels. a) HRP-crosslinking preparation method for the generation of the SF hydrogels. In aqueous solution, CaO_2 will break down into $Ca(OH)_2$, H_2O_2, and O_2. H_2O_2 will be the substrate for the HRP-mediated crosslinking of SF tyrosine side chains, leading to hydrogels formation; b) SF structural analysis by Transmission Electron Microscopy (TEM) after 7 days of hydrogels post-gelation. Scale bar: 200 nm; c) SF hydrogels microstructure analysis by Cryo-Scanning Electron Microscopy (Cryo-SEM) after 7 days of hydrogels post-gelation. Scale bar: 1 μm; d) X-ray diffraction (XRD) analysis after 1, 3, 7, 10, and 14 days of hydrogels post-gelation; e) SF hydrogels modulus versus time of gelation; f) SF hydrogels' pH responsiveness after 2 h of immersion in 0.154 M NaCl aqueous solution at pH 3, 7.4 and 10.5; g) Doxorubicin release profile of SF hydrogels immersed in phosphate buffered saline (PBS) after 3, 6, 12, 24, h and 3, 7, 14 days.

solubility of SF in acidic pH and loss of water molecules from the hydrogels induced by the ionic forces of the low pH condition. On the other side, the hydrogels responsiveness was not affected by physiological or basic pH conditions, showing stable structural properties. This behavior does not resemble the one seen in previously developed hydrogels using SF 16 wt%, which responded by their swelling when immersed in basic pH conditions.[22] This can be related to the fact that the hydrogels herein developed possess a higher degree of crosslinking, preventing hydrogels swelling in neutral and basal conditions.

In the optics of anticancer drug-releasing systems, the DOX release profile from SF hydrogels was investigated by means of soaking the DOX-loaded SF hydrogels in PBS for up to 14 days (Figure 1g). A low DOX release profile was observed for all the formulations during the initial 7 days of testing. After 14 days, Ca-1 hydrogels showed a higher level of DOX release than Ca-2, which could be due to the earlier degradation of Ca-1 (Figure S2, Supporting Information). In fact, it has been demonstrated that a higher CaO_2 concentration reduces hydrogels' degradation rate.[23] As compared to the calcium-containing SF hydrogels, the control H_2O_2 showed instead a notable increase of the DOX released level after 14 days, possibly related with an initial hydrogels degradation and the larger pores size, as compared to the calcium ones. The compacted porous microstructure of the calcium-containing SF hydrogels (Figure 1c) can also provide an explanation of the observed low DOX release. Pores being smaller than 1 μm (Ca-1: 0.216 ± 0.031 μm; Ca-2: 0.169 ± 0.023 μm), and hydrogels high crystallinity, impede the fast release of the drug. Therefore, this aspect can be very interesting in the context of controlled release profile of drugs,[2,3] enabling to go from a fast to slow release.

The in vitro cell encapsulation within the proposed hydrogels was explored using an osteosarcoma SaOs-2 human cell line, following the procedure represented in **Figure 2**a. Cell viability and proliferation of encapsulated SaOs-2 tumor cells were evaluated by Alamar blue (Figure 2b) and DNA quantification (Figure 2c). In all formulations, it was possible to observe that until day 3 cells presented a stable metabolic activity (Figure 2b). However, after 10 ($p < 0.001$) and 14 ($p < 0.001$) days of culturing, a significant decrease in metabolic activities of the cells was detected. This is concomitant with the SF hydrogels' β-sheet conformation transition, which demonstrated already in a previous work to reduce cells viability and induce apoptosis.[32] Results obtained from DNA quantification (Figure 2c) confirmed the effect of hydrogels crystallinity on cells behavior by the significant decrease in cell proliferation after 10 days of culturing ($p < 0.001$). A possible explanation to this phenomenon could be related with the compacted hydrogels structure after the change of conformation, which impaired the nutrients and oxygen exchanges and thus compromised the cells viability.

Given the importance of angiogenesis in tumor formation,[33] the angiogenic potential of SF hydrogels was assessed through an in ovo CAM assay. The angiogenic response was semiquantitatively evaluated (Figure 2d) following the procedure described by Silva-Correia et al.,[34] and was also qualitatively evaluated by H&E and lectin histological staining (Figure 2e). From the quantification of blood vessels convergence (Figure 2d), it was noticed that all SF hydrogels formulations possessed a statistically higher number (Ca-1 $p < 0.01$, Ca-2 $p < 0.05$, H_2O_2 $p < 0.001$) of convergent blood vessels, as compared to the gelatin sponge used as negative control. However, no significant differences were observed among the different SF hydrogels formulations tested, and between SF hydrogels and the filter paper used as positive control. From the CAM H&E histological analysis (Figure 2e), it was observed that the calcium-containing SF hydrogels (and the control ones) were partially reabsorbed by the CAM membrane during the incubation time, due to the triggered inflammatory response. Moreover, from the H&E and lectin staining (Figure 2e), it was possible to observe that the SF hydrogels (both using CaO_2 and H_2O_2 as oxidizer) do not allow surrounding tissue and almost no endothelial cells infiltration (black arrows in Figure 2e), contrarily to the FP controls. The obtained angiogenic profile could be related to the highly compacted microstructure of these hydrogels, even after 4 days of preparation (where they should have a more amorphous conformation), in which endothelial cells are not allowed to infiltrate. Further Cryo-SEM analysis of the hydrogels after 4 days of preparation could verify this hypothesis.

The calcium-containing SF hydrogels were ultimately evaluated by subcutaneous implantation in CD1 and nude CD1 (NCD1) mice models, for screening the in vivo biostability and biocompatibility up to 6 weeks (**Figure 3**). After 3- and 6-weeks post-implantation, it was possible to see that all the SF formulations, without and with SaOs-2 cancer cells encapsulation, were stably present in the connective tissue and no chronic inflammation was observed. From the TUNEL staining it was noticed an increased cells death surrounding the SF hydrogels, particularly on those crosslinked with CaO_2 (controls shown in Figure S3, Supporting Information). This observation can be related to the presence of calcium ions composing the hydrogels, confirmed with energy-dispersive x-ray spectroscopy (EDS) analysis with values going from 2.4 wt% in the Ca-1 and 4.1 wt% in the Ca-2 (data not shown), which can possibly trigger the cell apoptotic process.[35]

In summary, in this study, we developed novel HRP-crosslinked SF hydrogels using calcium peroxide (CaO_2) as substrate. For comparison purposes, these hydrogels were compared with HRP-crosslinked hydrogels using hydrogen peroxide (H_2O_2) crosslinking. The calcium-containing SF hydrogels were generated in random-coil conformation, and spontaneously acquired β-sheet conformation over time. A compacted porous microstructure was observed in all hydrogel formulations, with special relevance for the calcium-containing SF hydrogels presenting desirable features for the spatio–temporal release of drugs. Their ionic stimuli responsiveness and rapid gelation time allowed the encapsulation and viability of SaOs-2 cells up to 10 days of culture. However, the calcium-containing SF hydrogels conversion into a crystalline β-sheet conformation affected cells metabolic activity and proliferation. Preliminary in ovo and in vivo data showed calcium-containing SF hydrogels' abilities to inhibit angiogenesis and mediate cells death, respectively, providing new ambitions to explore these 3D in vitro matrices for novel antitumor therapeutic strategies. In fact, thanks to these hydrogels capability to fast jellify at physiological conditions, they could be loaded with therapeutics and injected in the patient in the tumor site, thus acting as in situ drug-releasing systems. In addition, thanks to their capabilities to induce tumor cells death upon β-sheet induction

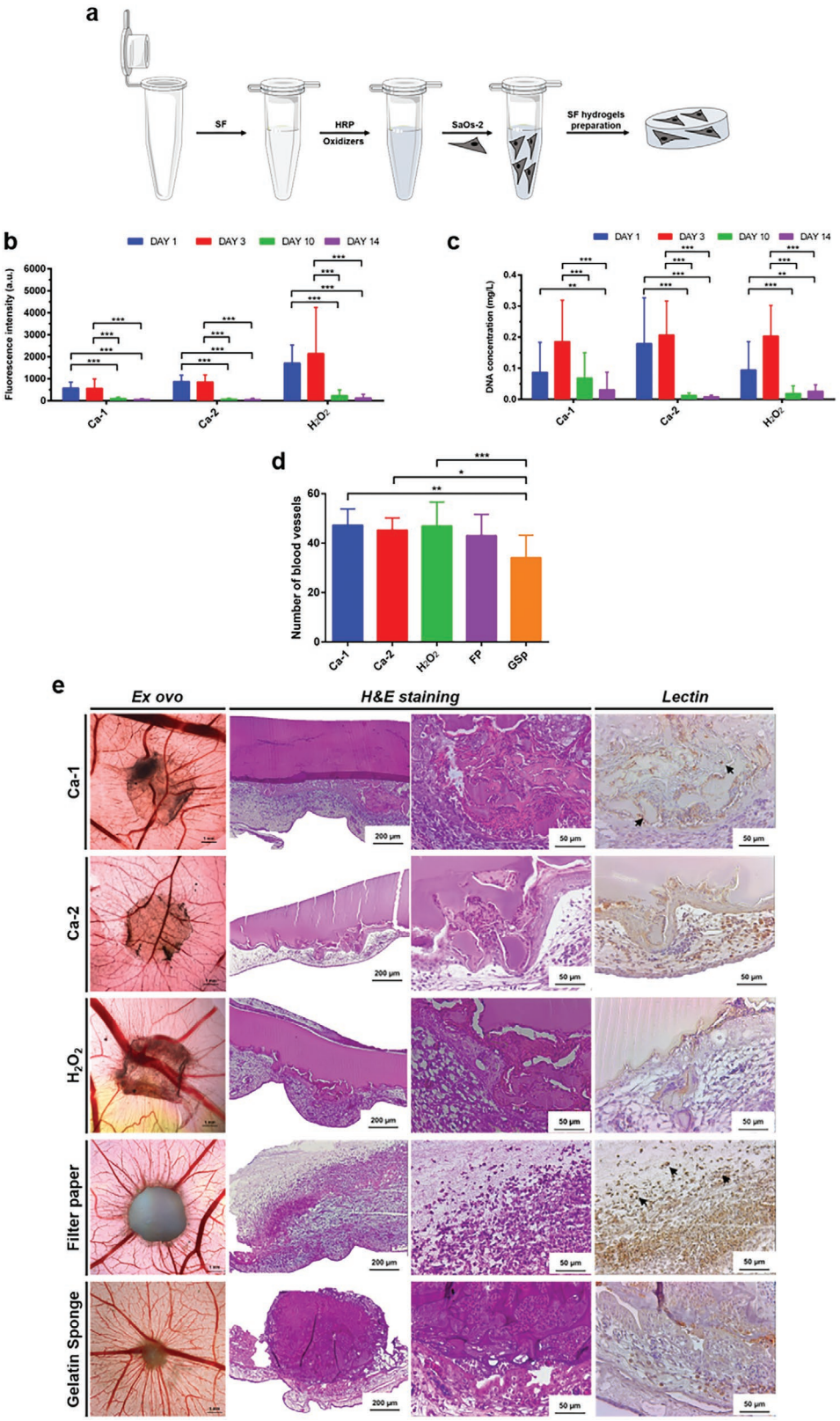

Figure 2. In vitro cell behavior and angiogenic potential of HRP-crosslinked SF hydrogels. a) SaOs-2 encapsulation method into SF hydrogels; b) Alamar blue metabolic activity and c) DNA quantification of encapsulated SaOs-2 cancer cells after 1, 3, 10, and 14 days of culturing; d) Number of converging blood vessels toward the SF hydrogels implanted in the CAM for 4 days. Filter paper (FP) and gelatin sponge (GSp) were used, respectively, as positive and negative controls. e) Ex ovo images, H&E and lectin staining of SF hydrogels implanted in the CAM for 4 days.

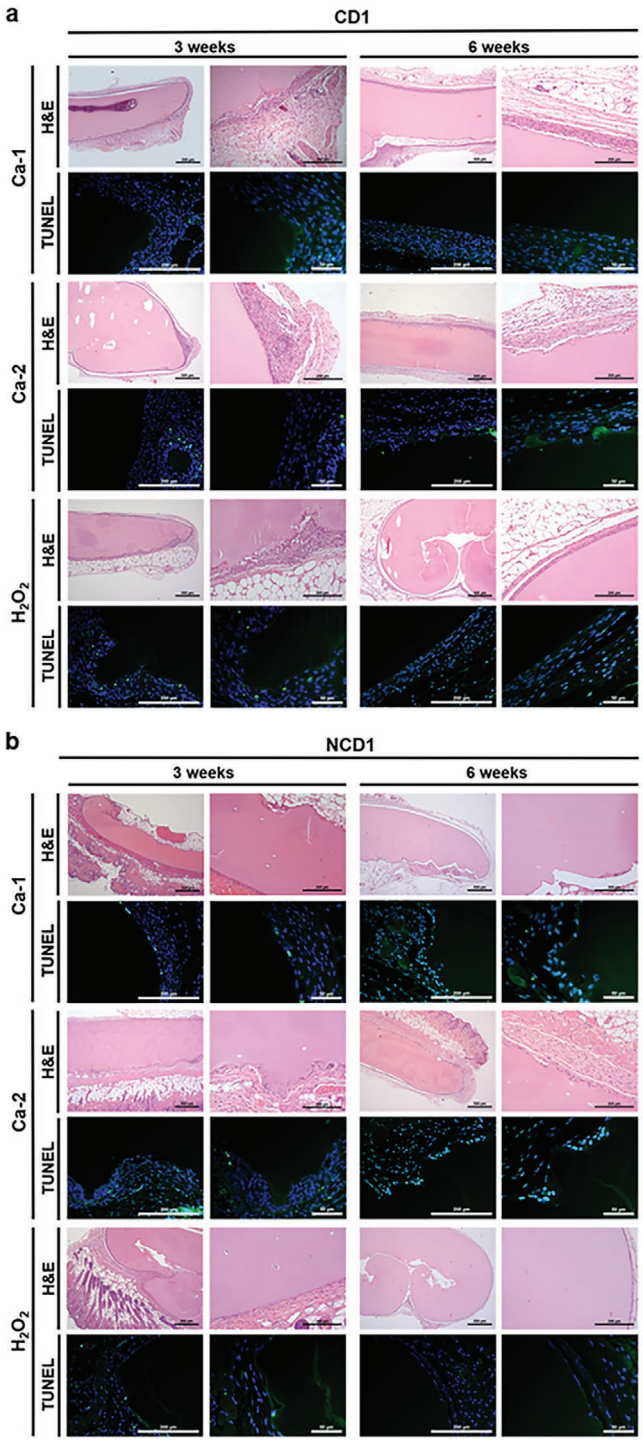

Figure 3. In vivo subcutaneous implantation of SF hydrogels in a) CD1 and b) nude NCD1 mice. Images show representative explant regions stained with H&E and TUNEL.

and to inhibit angiogenesis, they could enhance the antitumor effect, by impairing nutrients and blood supplies. In this way, the calcium-containing SF hydrogels could be used as neoadjuvant therapy systems prior to surgery, by reducing the tumor mass and giving clearer tumor-free margins, thus reducing the overall treatments side effects.

Experimental Section

The maintenance and use of animals were performed in accordance to the European Council Directives on Animal Care (Directive 2010/63/EU) and were approved by the Ethics Committee of University of Minho and by the Portuguese Licensing Authority (DGV-DSSPA).

The Experimental section details can be found in the Supporting Information.

Supporting Information

Supporting Information is available from the Wiley Online Library or from the author.

Acknowledgements

L.P. thanks the International mobility program of the University of Trento, Italy. J.S.-C. and J.M.O. thank the Portuguese Foundation for Science and Technology (FCT) for the funds provided under the program Investigador FCT 2015 (IF/00115/2015 and IF/01285/2015, respectively). This research was funded by Norte Portugal Regional Operational Programme (NORTE 2020), under the PORTUGAL 2020 Partnership Agreement, through the European Regional Development Fund (ERDF) (NORTE-01-0145-FEDER-000023). The project BAMOS (H2020-MSCA-RISE-2016-734156) funded by the European Union under the Horizon 2020 program, and the EU Framework Programme for Research and Innovation H2020 on FoReCaST (Grant Agreement No.668983), are also greatly acknowledged. V.P.R. acknowledge for the Junior Researcher contract (POCI-01-0145-FEDER-031367) attributed by the Portuguese Foundation for Science and Technology to Fun4TE project (PTDC/EMD-EMD/31367/2017). L.P. thanks C. Gonçalves for helping with analysis of rheology data, and T. Oliveira for the histology.

Conflict of Interest

The authors declare no conflict of interest.

Data Availability Statement

Research data are not shared.

Keywords

bone, calcium, cancer, hydrogels, silk fibroin

Received: December 14, 2020
Revised: January 8, 2021
Published online:

[1] C. C. Huang, W. T. Chia, M. F. Chung, K. J. Lin, C. W. Hsiao, C. Jin, W. H. Lim, C. C. Chen, H. W. Sung, *J. Am. Chem. Soc.* **2016**, *138*, 5222.
[2] L.-P. Yan, J. M. Oliveira, A. L. Oliveira, R. L. Reis, *J. Tissue Eng. Regener. Med.* **2016**, *11*, 3168.

[3] H. Wu, S. Liu, L. Xiao, X. Dong, Q. Lu, D. L. Kaplan, *ACS Appl. Mater. Interfaces* **2016**, *8*, 17118.
[4] S. A. Kamba, M. Ismail, S. H. Hussein-Al-Ali, T. A. T. Ibrahim, Z. A. B. Zakaria, *Molecules* **2013**, *18*, 10580.
[5] G. Chang, Y. Chen, Y. Li, S. Li, F. Huang, Y. Shen, A. Xie, *Carbohydr. Polym.* **2015**, *122*, 336.
[6] C. Y. Liaw, S. Ji, M. Guvendiren, *Adv. Healthcare Mater.* **2018**, *7*, 1701165.
[7] S. Hinderer, S. L. Layland, K. Schenke-Layland, *Adv. Drug Delivery Rev.* **2016**, *97*, 260.
[8] B. Kundu, R. Rajkhowa, S. C. Kundu, X. Wang, *Adv. Drug Delivery Rev.* **2013**, *65*, 457.
[9] D. N. Rockwood, R. C. Preda, T. Yücel, X. Wang, M. L. Lovett, D. L. Kaplan, *Nat. Protoc.* **2011**, *6*, 1612.
[10] S. Midha, S. Murab, S. Ghosh, *Biomaterials* **2016**, *97*, 133.
[11] Y. Jin, B. Kundu, Y. Cai, S. C. Kundu, J. Yao, *Colloids Surf., B* **2015**, *134*, 339.
[12] A. M. Sitarski, H. Fairfield, C. Falank, M. R. Reagan, *ACS Biomater. Sci. Eng.* **2018**, *4*, 324.
[13] V. Krishnan, E. A. Vogler, A. M. Mastro, *J. Cell. Biochem.* **2015**, *116*, 2715.
[14] F. Salamanna, D. Contartese, M. Maglio, M. Fini, *Oncotarget* **2016**, *7*, 44803.
[15] R. L. Siegel, K. D. Miller, A. Jemal, *Ca-Cancer J. Clin.* **2017**, *67*, 7.
[16] American Cancer Society, Cancer Facts & Figures 2017, Atlanta: American Cancer Society **2017**.
[17] E. Ward, C. Desantis, A. Robbins, B. Kohler, A. Jemal, *Ca Cancer J. Clin.* **2014**, *64*, 83.
[18] T. M. Jackson, M. Bittman, L. Granowetter, *Curr. Probl. Pediatr. Adolesc. Health Care* **2016**, *46*, 213.
[19] K. Rickel, F. Fang, J. Tao, *Bone* **2017**, *102*, 69.
[20] A. Alfranca, L. Martinez-Cruzado, J. Tornin, A. Abarrategi, T. Amaral, E. De Alava, P. Menendez, J. Garcia-Castro, R. Rodriguez, *Cell. Mol. Life Sci.* **2015**, *72*, 3097.
[21] S. K. Denduluri, Z. Wang, Z. Yan, J. Wang, Q. Wei, M. K. Mohammed, R. C. Haydon, H. H. Luu, T. He, *J. Biomed. Res.* **2016**, *30*, 5.
[22] L.-P. Yan, J. Silva-Correia, V. P. Ribeiro, V. Miranda-Gonçalves, C. Correia, A. da Silva Morais, R. A. Sousa, R. M. Reis, A. L. Oliveira, J. M. Oliveira, R. L. Reis, *Sci. Rep.* **2016**, *6*, 31037.
[23] P. L. Thi, Y. Lee, D. L. Tran, T. T. Hoang Thi, K. M. Park, K. D. Park, *J. Mater. Chem. B* **2020**, 11033.
[24] B. P. Partlow, C. W. Hanna, J. Rnjak-Kovacina, J. E. Moreau, M. B. Applegate, K. A. Burke, B. Marelli, A. N. Mitropoulos, F. G. Omenetto, D. L. Kaplan, *Adv. Funct. Mater.* **2014**, *24*, 4615.
[25] F. Happey, A. J. Hyde, B. Manogue, *Biopolymers* **1967**, *5*, 749.
[26] M. K. Shah, K. Pramanik, *Afr. J. Biotechnol.* **2011**, *10*, 7878.
[27] Q. Lu, X. Hu, X. Wang, J. A. Kluge, S. Lu, P. Cebe, D. L. Kaplan, *Acta Biomater.* **2010**, *6*, 1380.
[28] G. M. Nogueira, M. A. De Moraes, A. C. D. Rodas, O. Z. Higa, M. M. Beppu, *Mater. Sci. Eng. C* **2011**, *31*, 997.
[29] M. Li, S. Lu, Z. Wu, K. Tan, N. Minoura, S. Kuga, *Int. J. Biol. Macromol.* **2002**, *30*, 89.
[30] M. A. de Moraes, G. M. Nogueira, R. F. Weska, M. M. Beppu, *Polymers* **2010**, *2*, 719.
[31] X. Chen, Z. Shao, D. P. Knight, F. Vollrath, *Proteins Struct. Funct. Bioinforma.* **2007**, *68*, 223.
[32] V. P. Ribeiro, J. Silva-Correia, C. Gonçalves, S. Pina, H. Radhouani, T. Montonen, J. Hyttinen, A. Roy, A. L. Oliveira, R. L. Reis, J. L. Oliveira, *PLoS One* **2018**, *13*, e0194441.
[33] S. M. Weis, D. A. Cheresh, *Nat. Med.* **2011**, *17*, 1359.
[34] J. Silva-Correia, V. Miranda-Gonçalves, A. J. Salgado, N. Sousa, J. M. Oliveira, R. M. Reis, R. L. Reis, *Tissue Eng., Part A* **2012**, *18*, 1203.
[35] S. Orrenius, B. Zhivotovsky, P. Nicotera, *Nat. Rev. Mol. Cell Biol.* **2003**, *4*, 552.